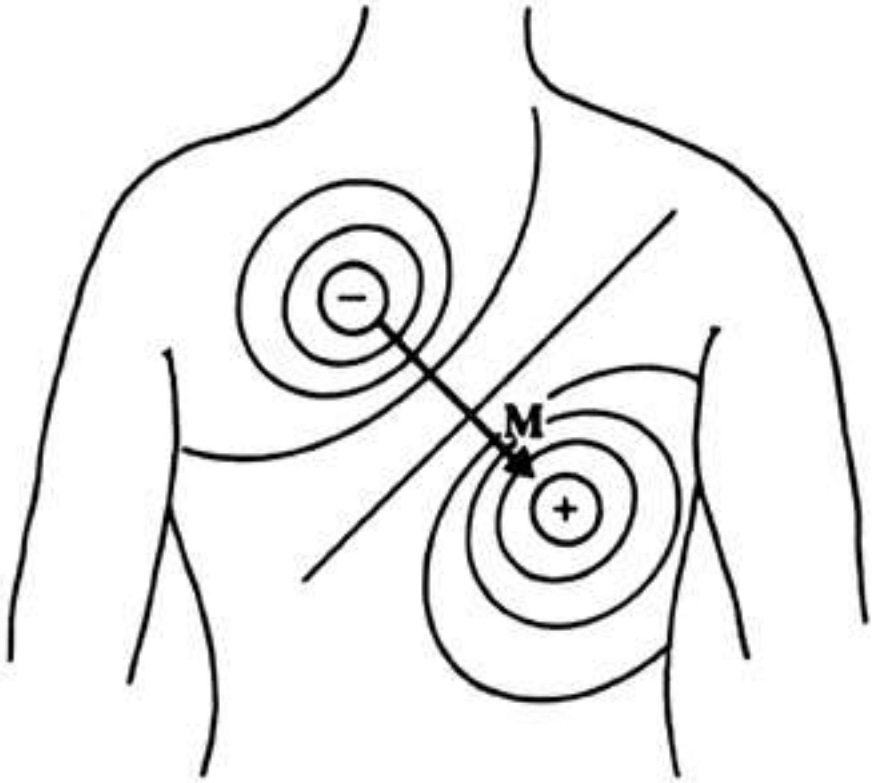

Figure 6.1 Rough sketch of the dipole field of the heart when the R wave is maximal
The dipole consists of the points of equal positive and negative charge separated from one another and denoted by the dipole moment vector **M**.

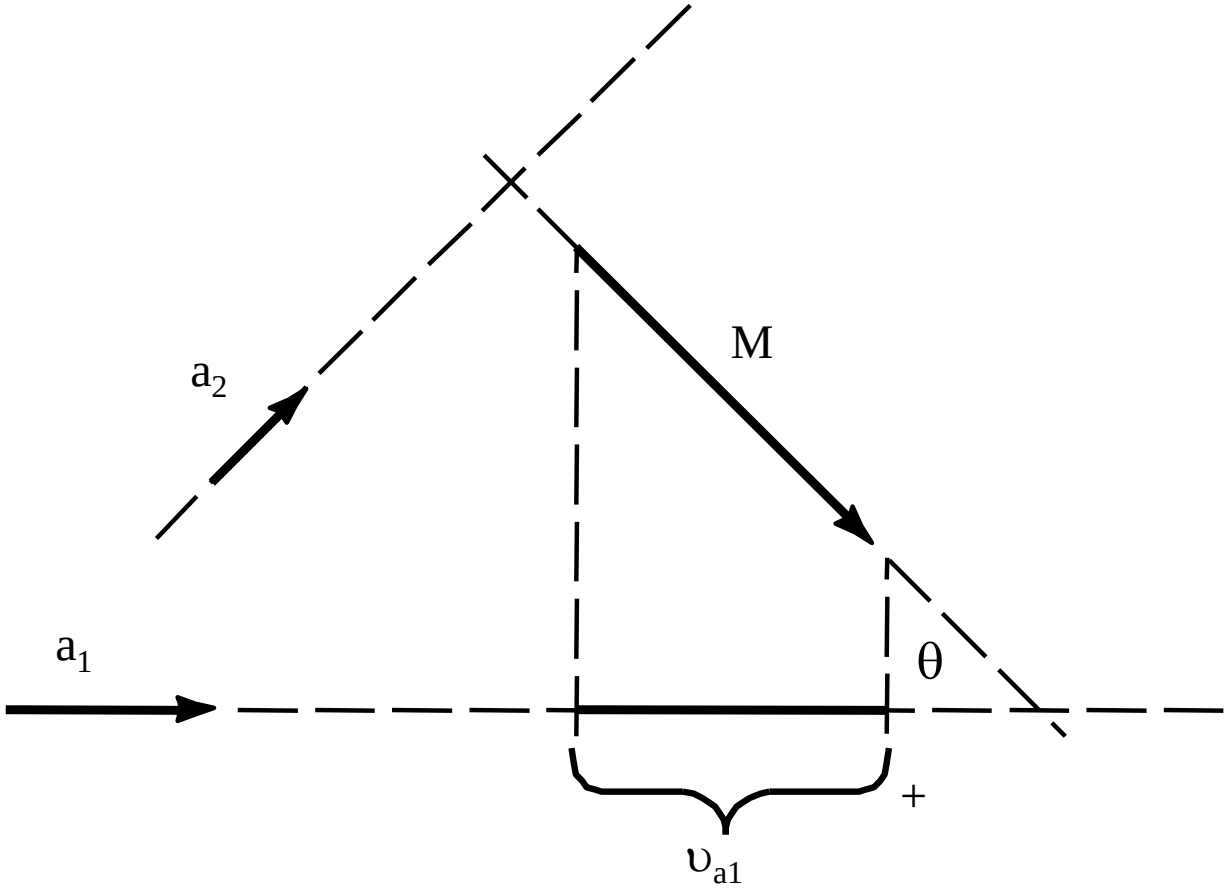

Figure 6.2 Relationships between the two lead vectors $\mathbf{a}_1$ and $\mathbf{a}_2$ and the cardiac vector **M**. The component of **M** in the direction of $\mathbf{a}_1$ is given by the dot product of these two vectors and denoted on the figure by v_{al}. Lead vector $\mathbf{a}_2$ is perpendicular to the cardiac vector, so no voltage component is seen in this lead.

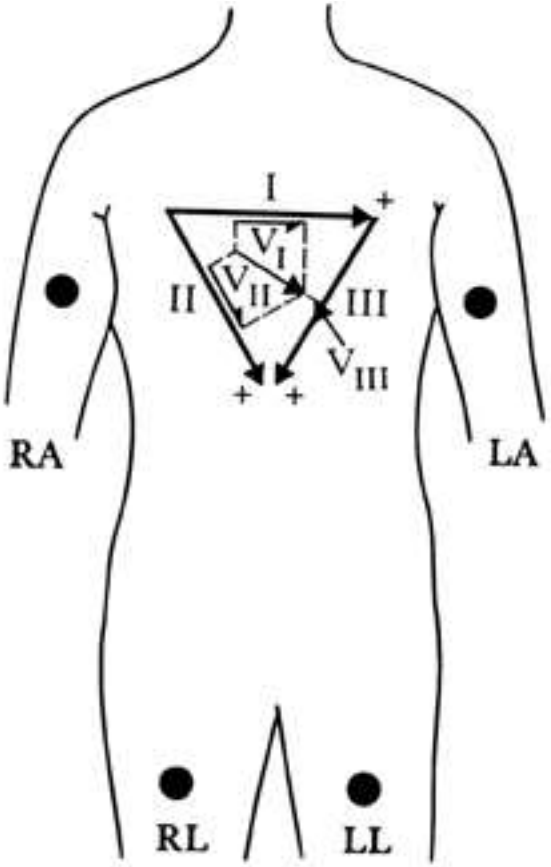

Figure 6.3 Cardiologists use a standard notation such that the direction of the lead vector for lead I is 0º, that of lead II is 60º, and that of lead III is 120º. An example of a cardiac vector at 30º with its scalar components seen for each lead is shown.

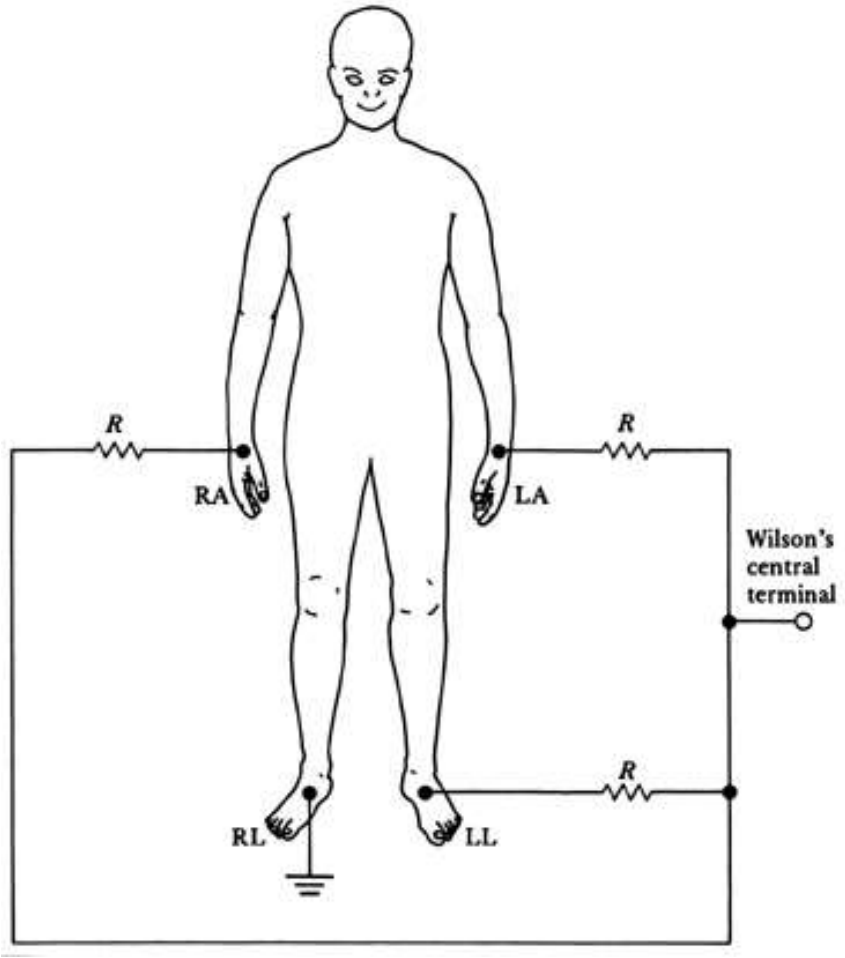

Figure 6.4 Connection of electrodes to the body to obtain Wilson's central terminal

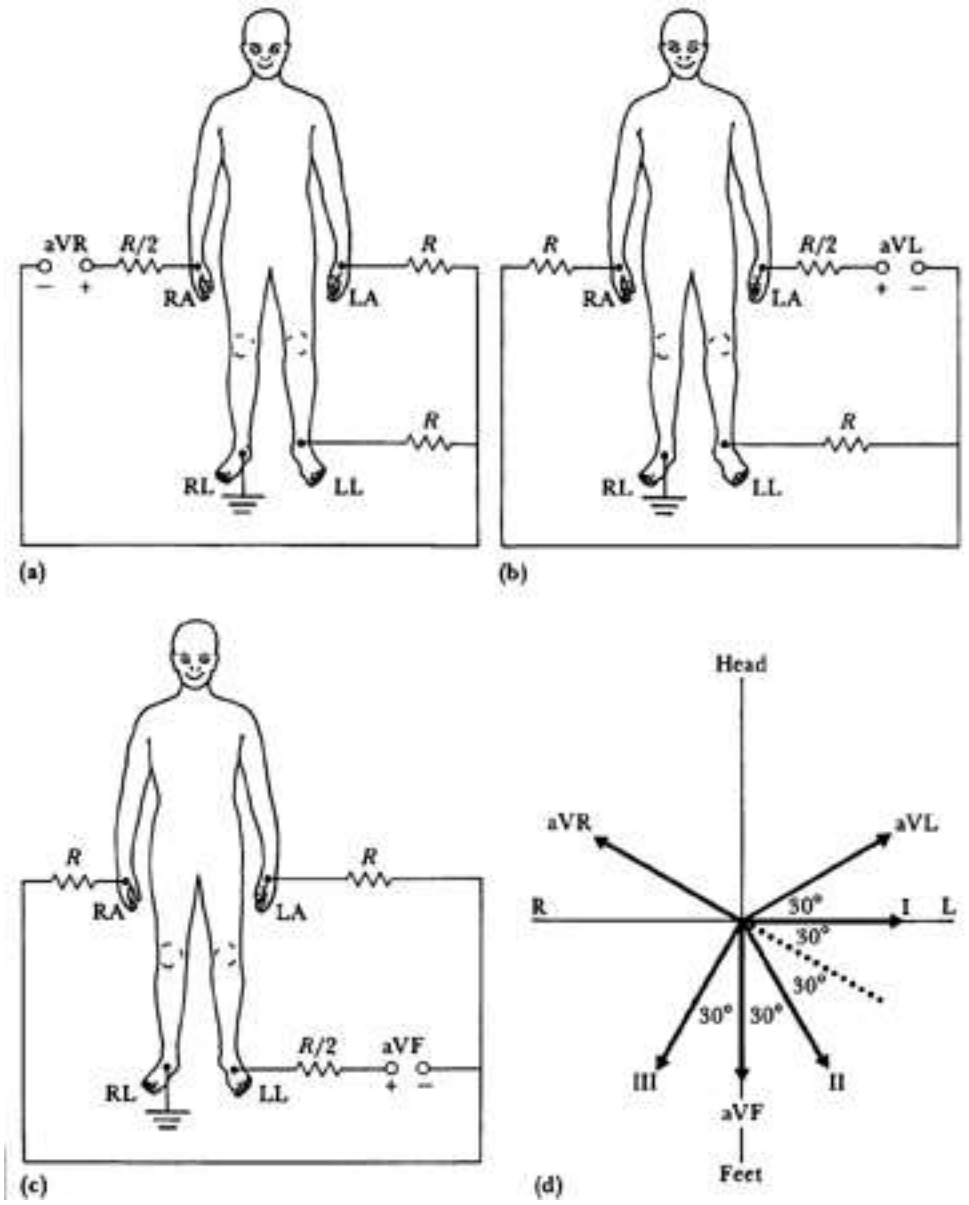

Figure 6.5 (a), (b), (c) Connections of electrodes for the three augmented limb leads. (d) Vector diagram showing standard and augmented lead-vector directions in the frontal plane.

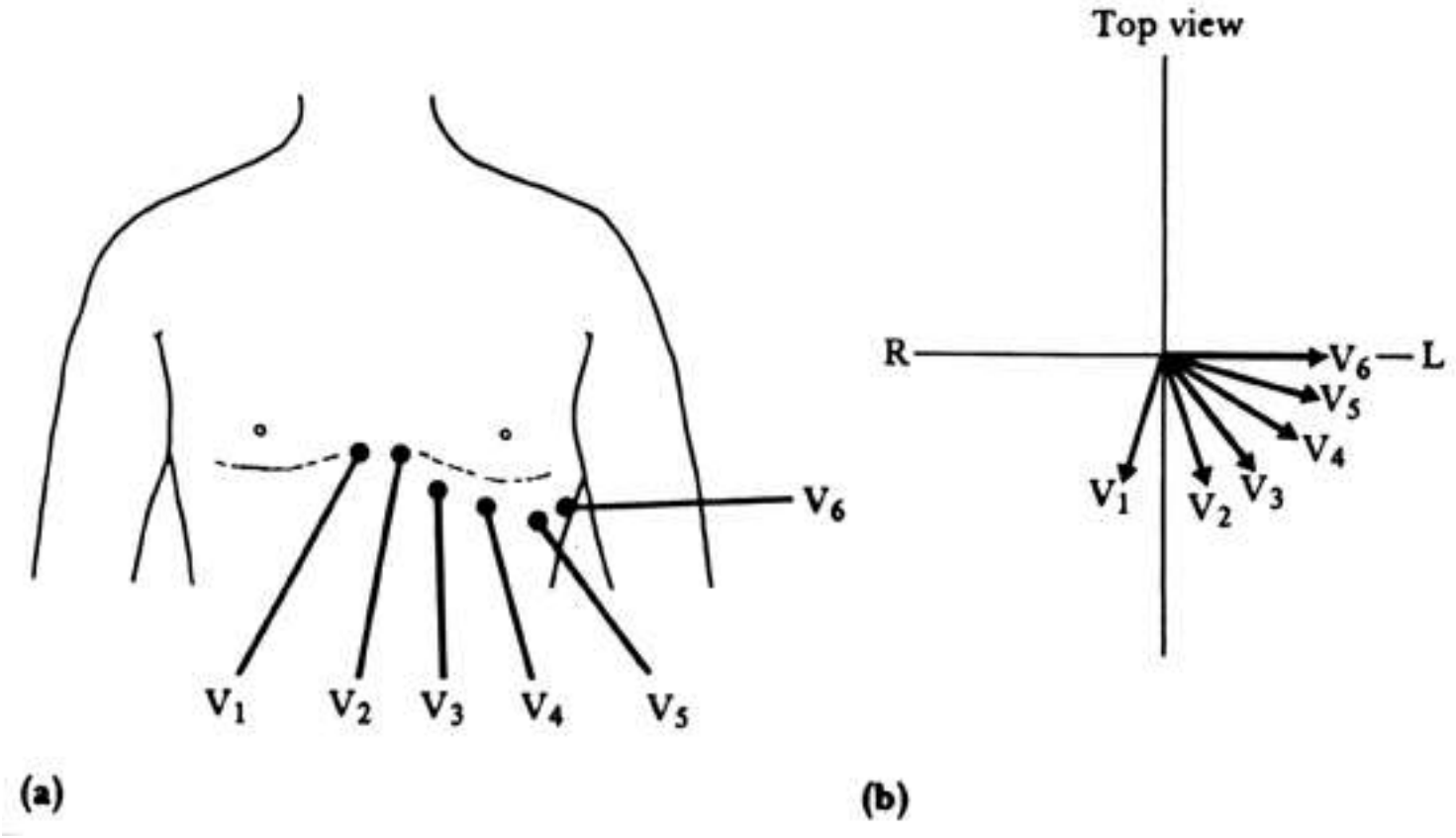

Figure 6.6 (a) Positions of precordial leads on the chest wall. (b) Directions of precordial lead vectors in the transverse plane.

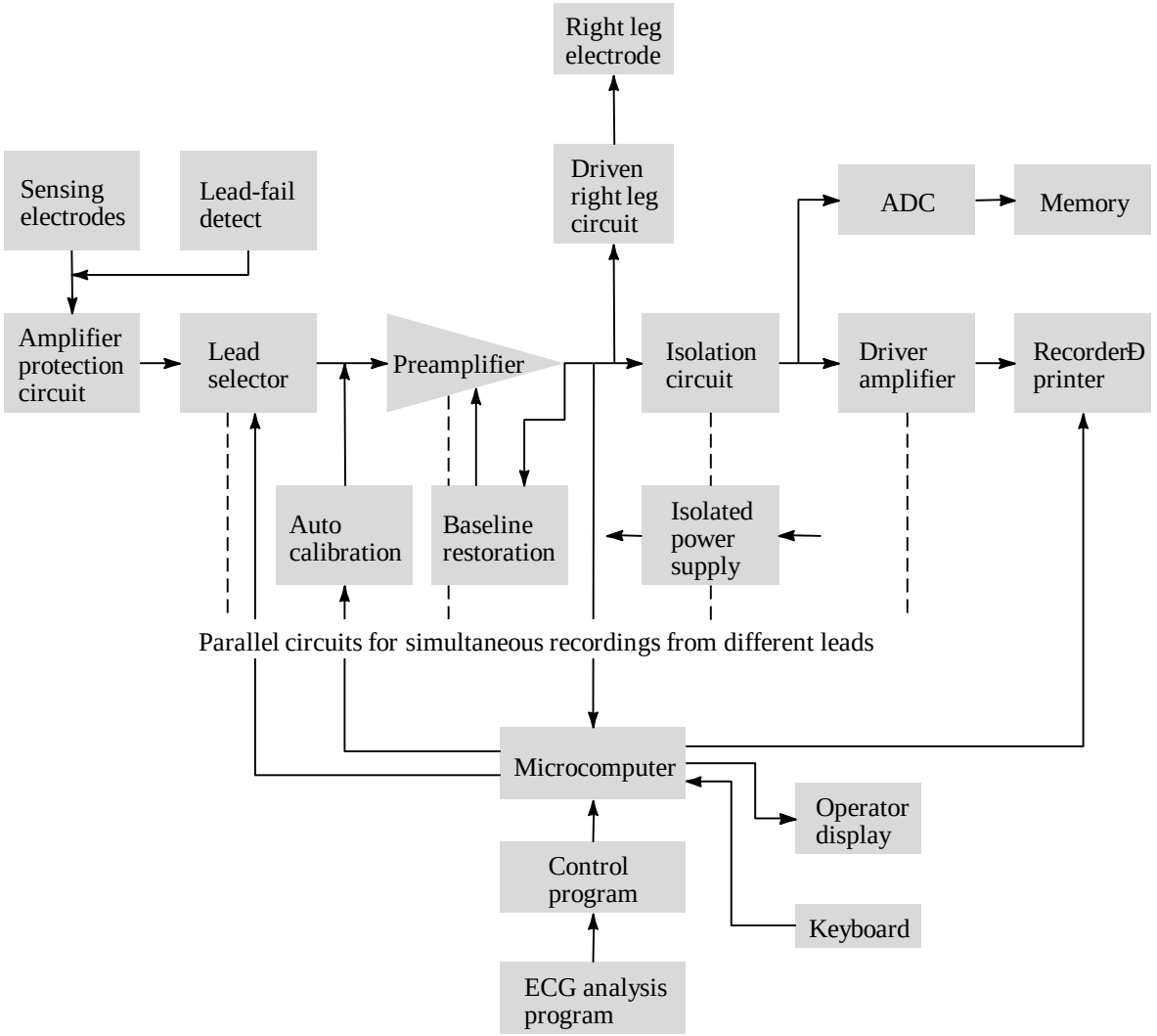

Figure 6.7 Block diagram of an electrocardiograph

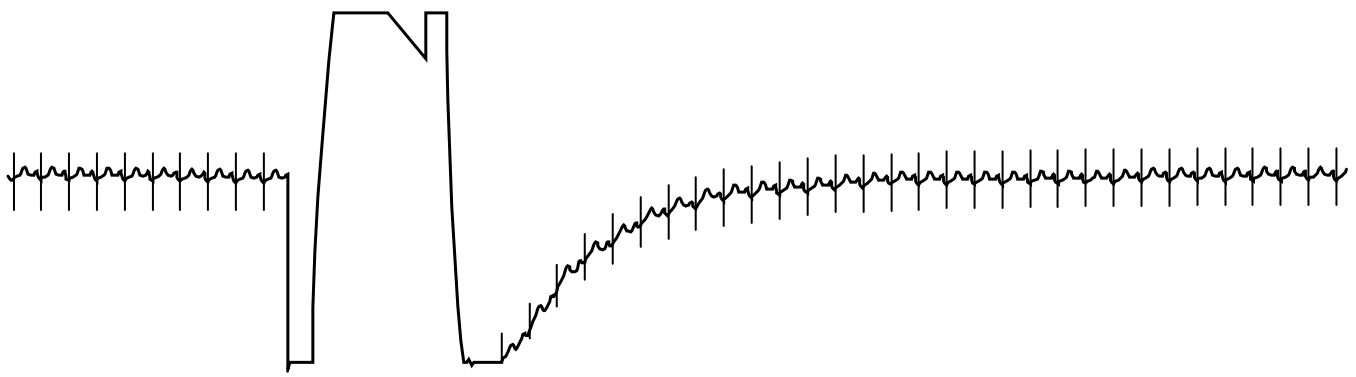

Figure 6.8 Effect of a voltage transient on an ECG recorded on an electrocardiograph in which the transient causes the amplifier to saturate, and a finite period of time is required for the charge to bleed off enough to bring the ECG back into the amplifier's active region of operation. This is followed by a first-order recovery of the system.

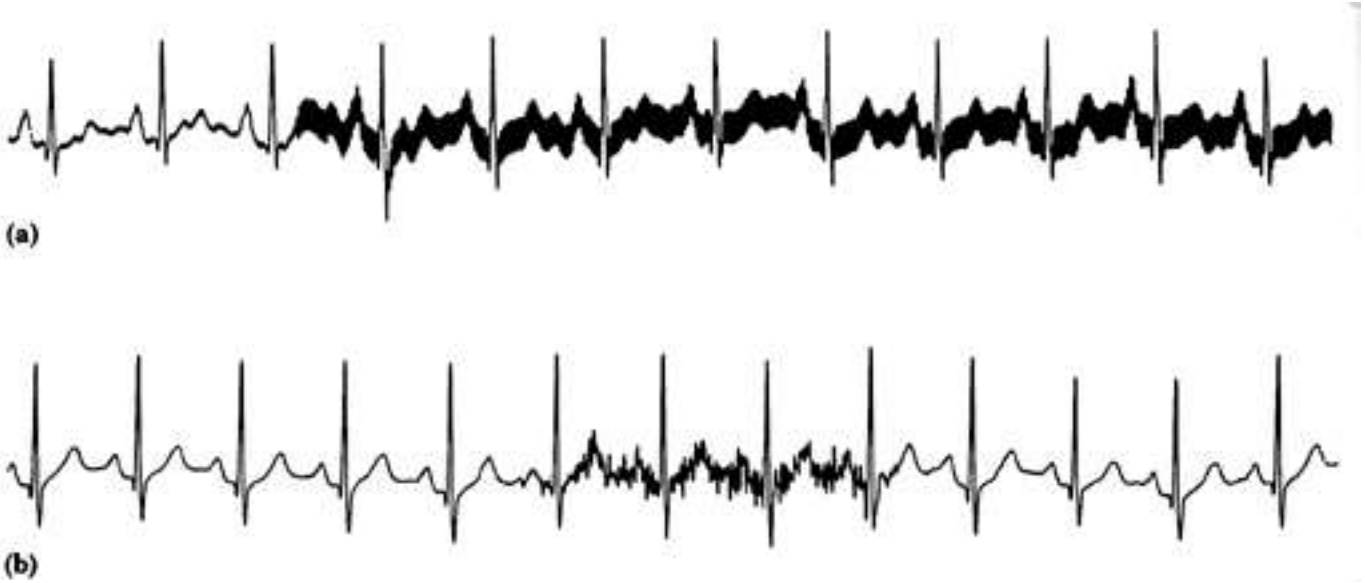

Figure 6.9 (a) 60 Hz power-line interference. (b) Electromyographic interference on the ECG. Severe 60 Hz interference is also shown on the bottom tracing in Figure 4.13.

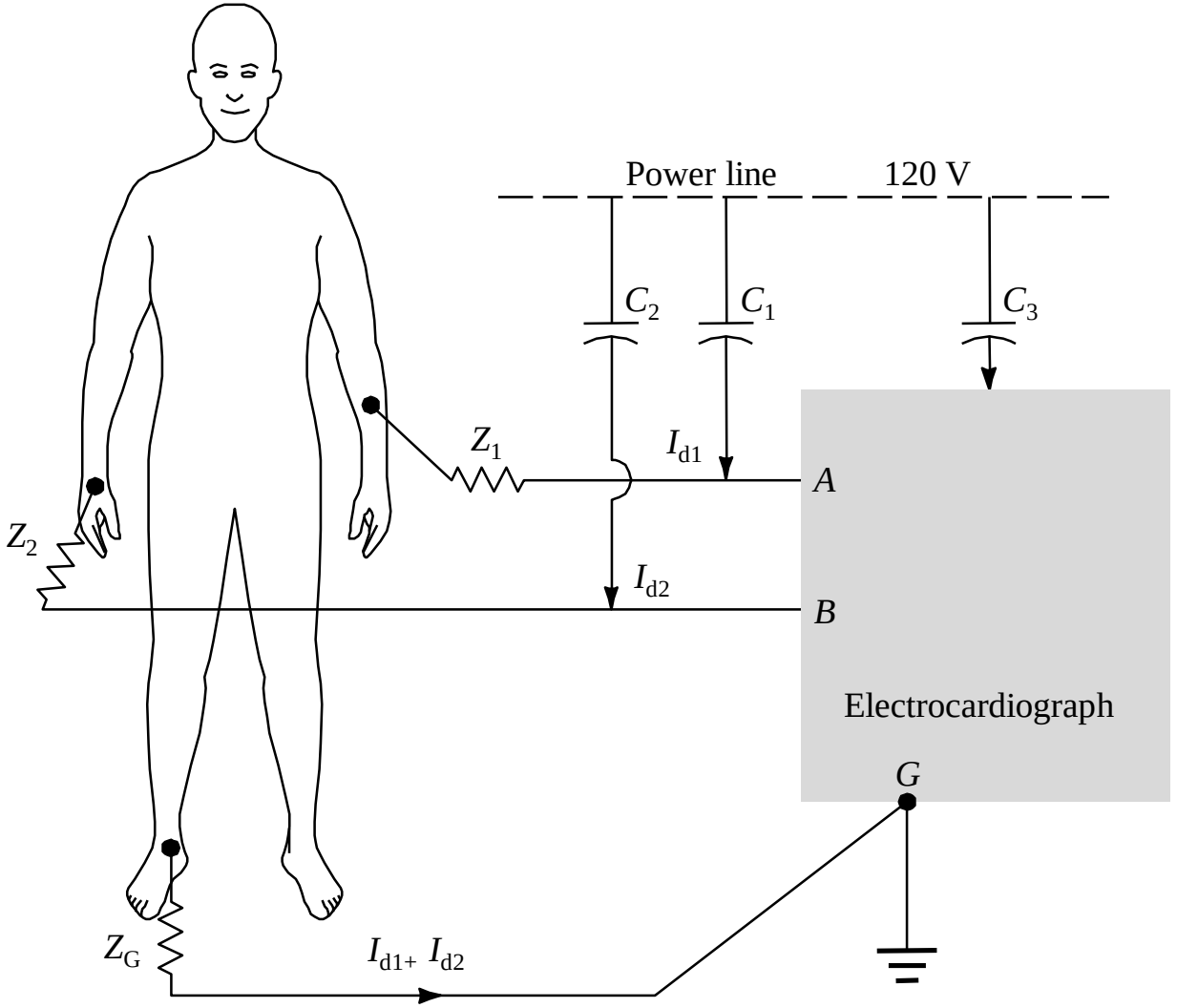

Figure 6.10 A mechanism of electric-field pickup of an electrocardiograph resulting from the power line. Coupling capacitance between the hot side of the power line and lead wires causes current to flow through skin-electrode impedances on its way to ground.

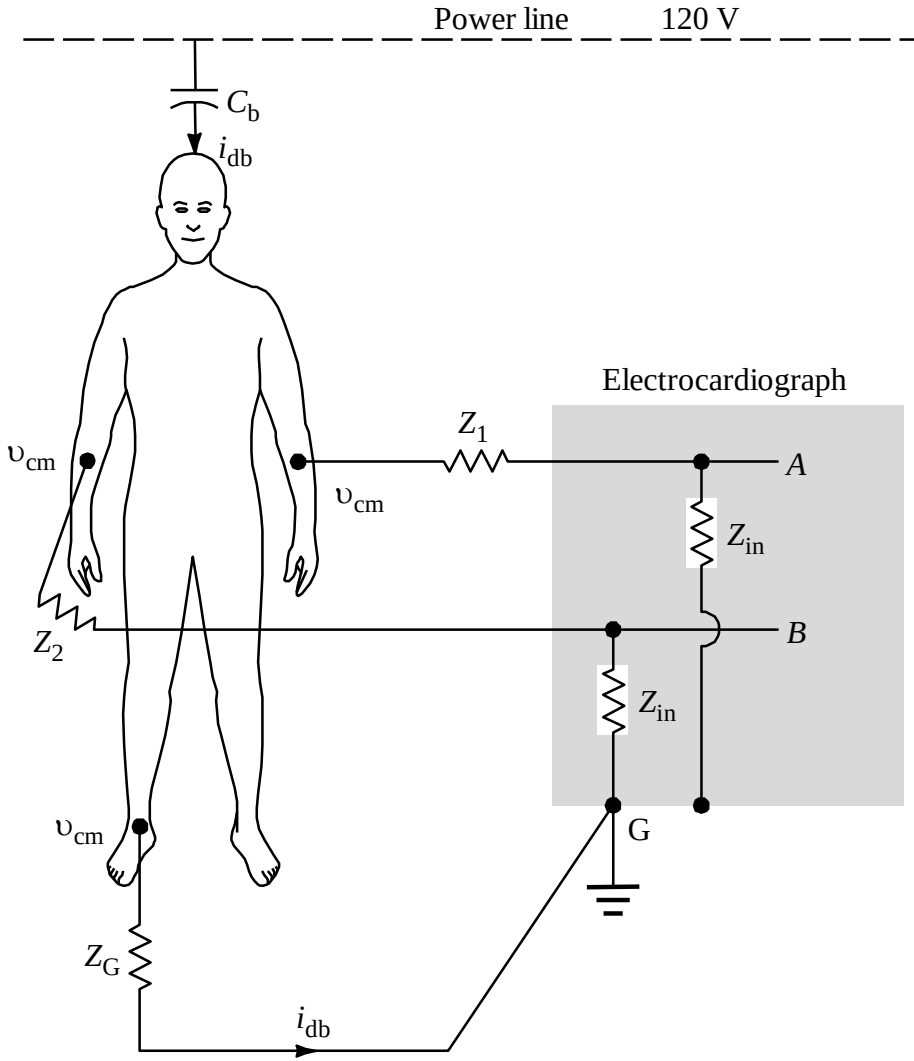

Figure 6.11 Current flows from the power line through the body and ground impedance, thus creating a common-mode voltage everywhere on the body. Z_{in} is not only resistive but, as a result of RF bypass capacitors at the amplifier input, has a reactive component as well.

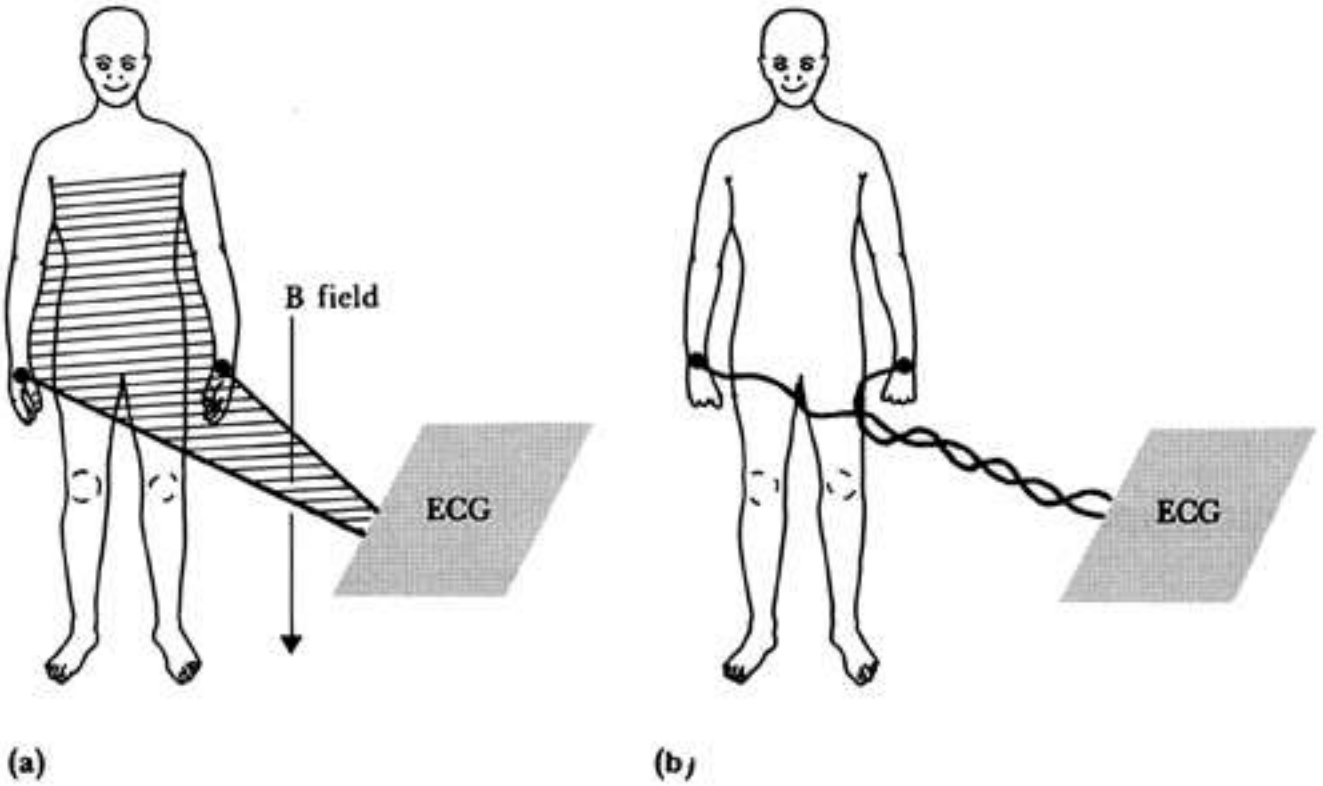

Figure 6.12 Magnetic-field pickup by the elctrocardiograph (a) Lead wires for lead I make a closed loop (shaded area) when patient and electrocardiograph are considered in the circuit. The change in magnetic field passing through this area induces a current in the loop. (b) This effect can be minimized by twisting the lead wires together and keeping them close to the body in order to subtend a much smaller area.

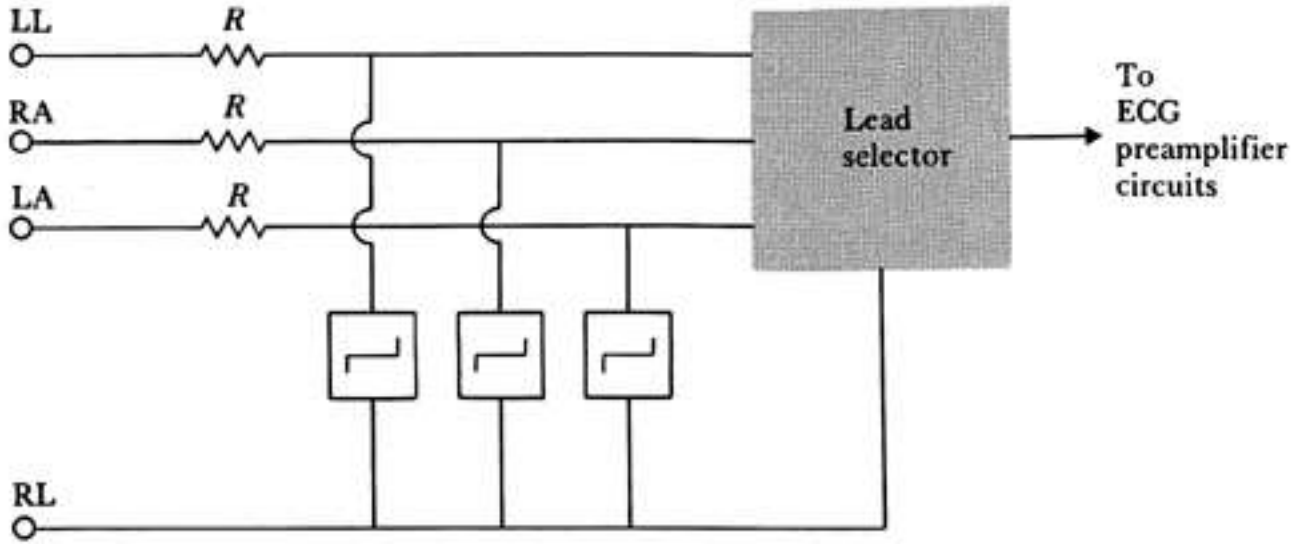

Figure 6.13 A voltage-protection scheme at the input of an electrocardiograph to protect the machine from high-voltage transients. Circuit elements connected across limb leads on left-hand side are voltage-limiting devices.

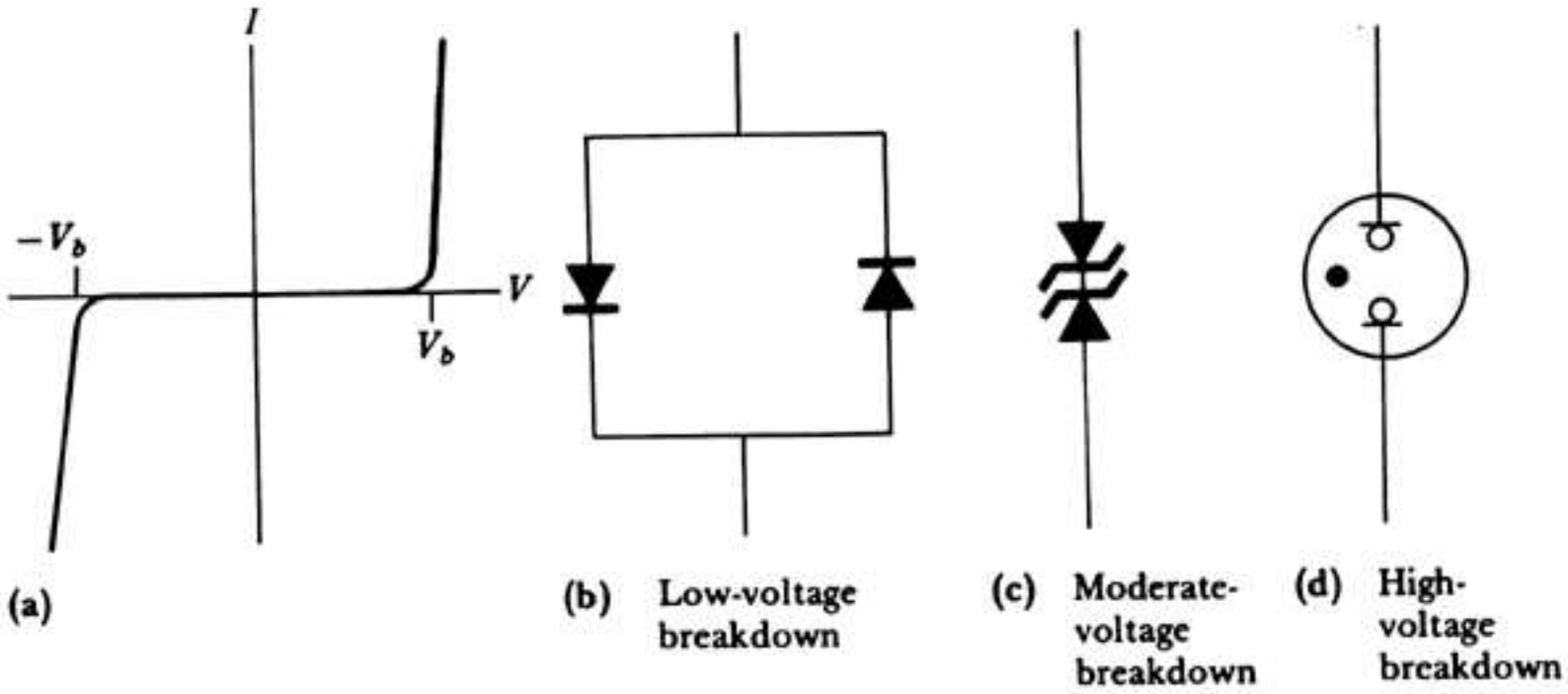

Figure 6.14 Voltage-limiting devices (a) Current-voltage characteristics of a voltage-limiting device. (b) Parallel silicon-diode voltage-limiting circuit. (c) Back-to-back silicon Zener-diode voltage-limiting circuit. (d) Gas-discharge tube (neon light) voltage-limiting circuit element.

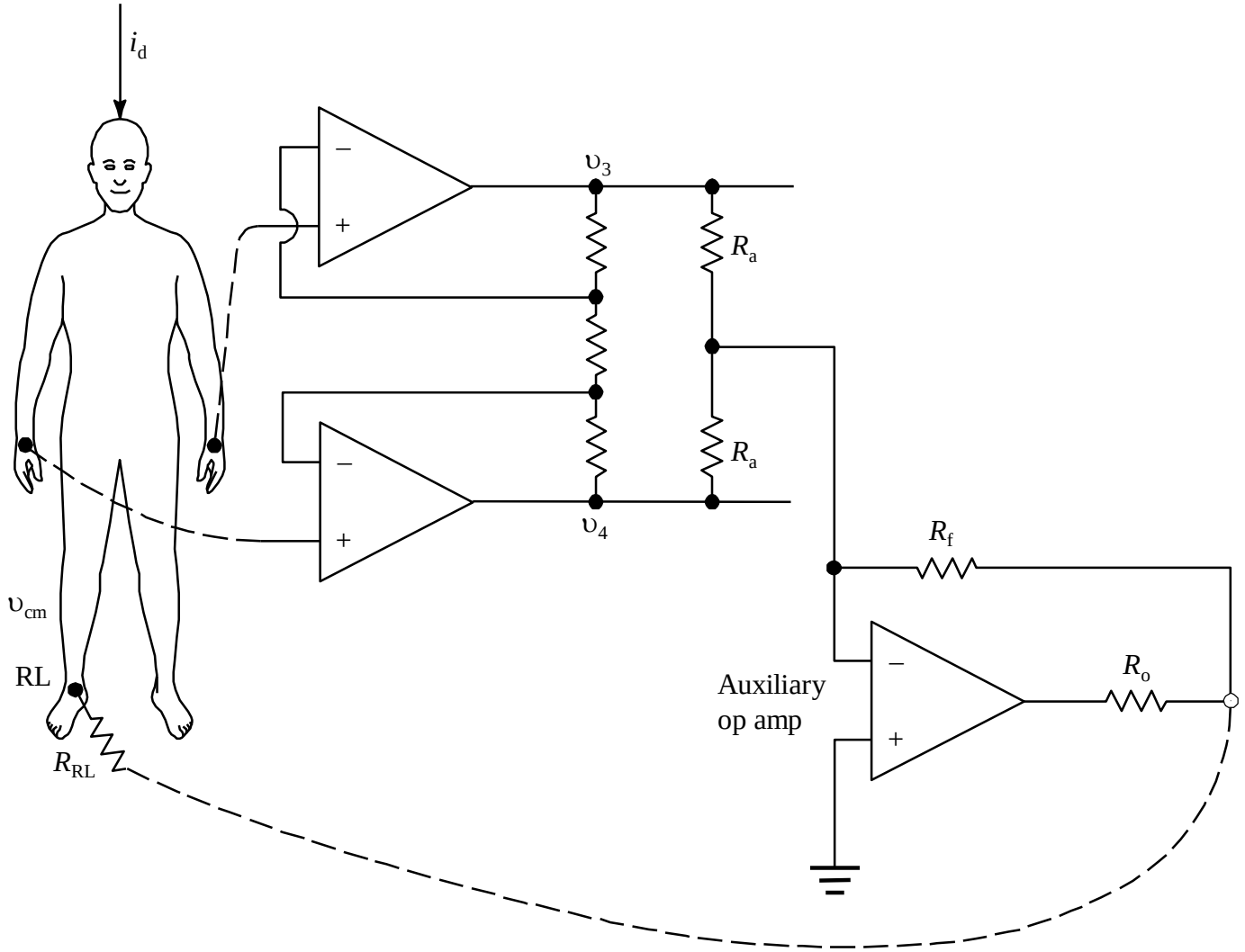

Figure 6.15 Driven-right-leg circuit for minimizing common- mode interference The circuit derives common-mode voltage from a pair of averaging resistors connected to v_3 and v_4 in Figure 3.5. The right leg is not grounded but is connected to output of the auxiliary op amp.

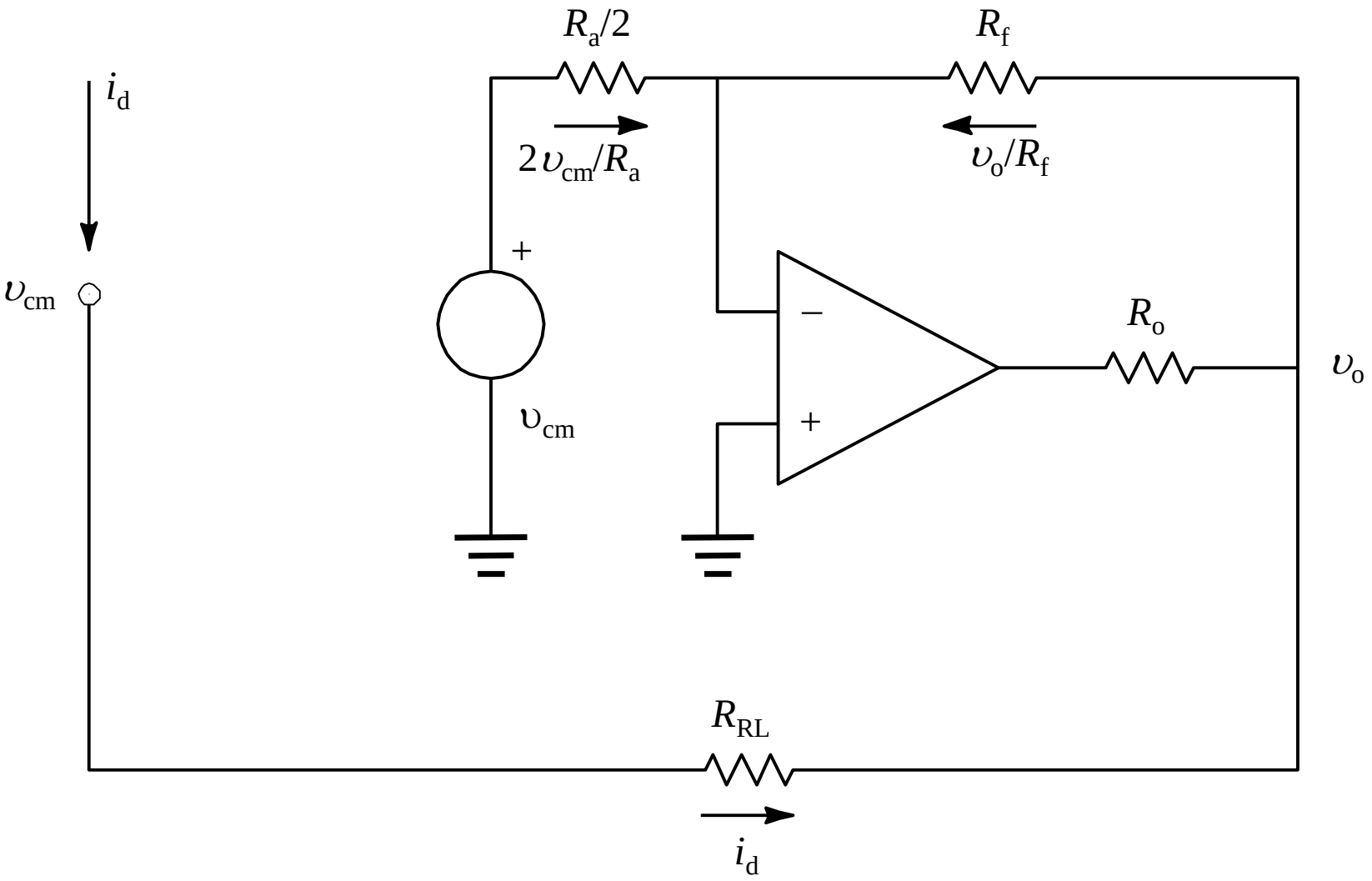

Figure E6.1 Equivalent circuit of driven-right-leg system of Figure 6.19.

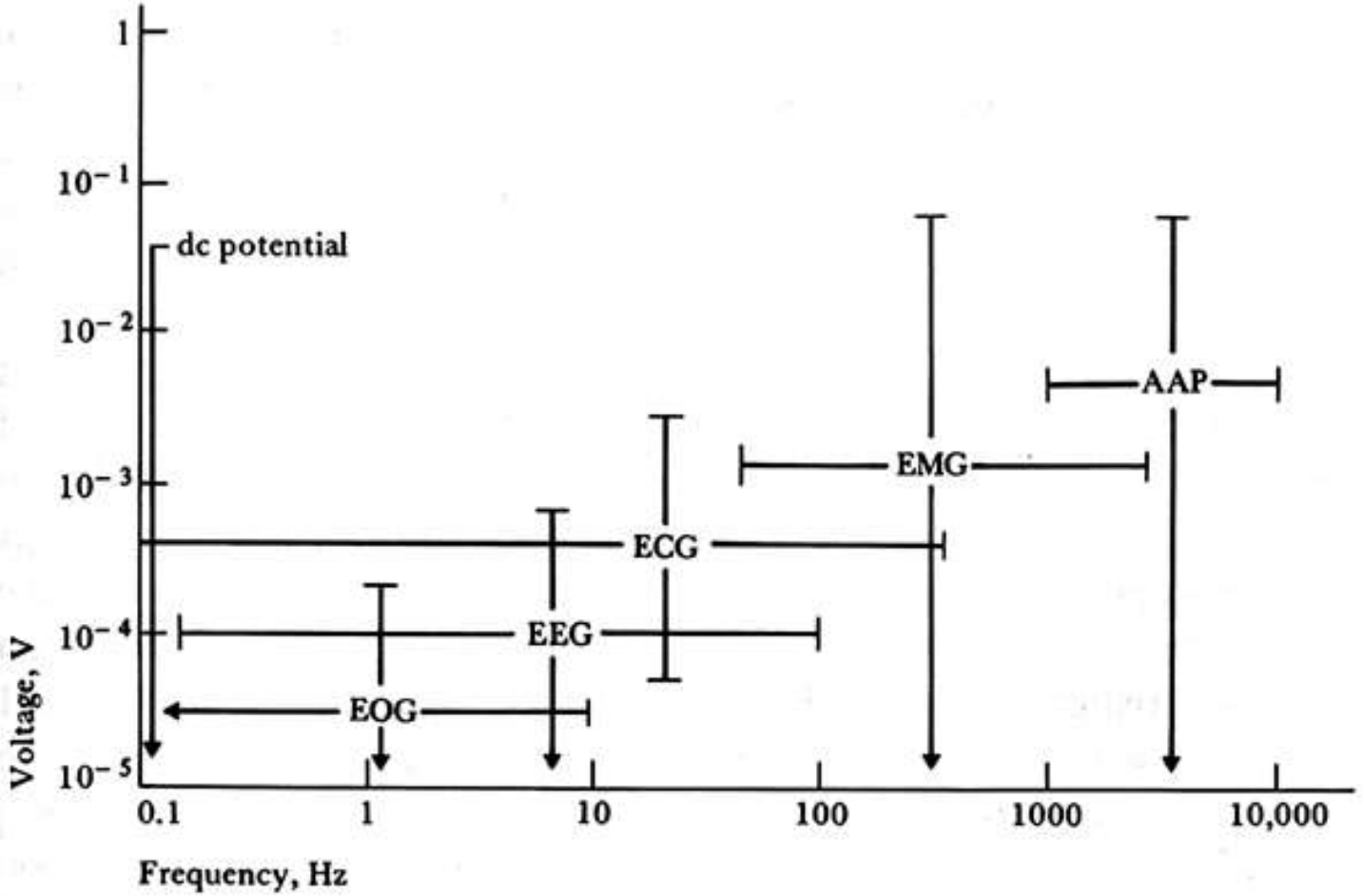

Figure 6.16 Voltage and frequency ranges of some common biopotential signals; dc potentials include intracellular voltages as well as voltages measured from several points on the body. EOG is the electrooculogram, EEG is the elctroencephalogram, ECG is the electrocardiogram, EMG is the electromyogram, and AAP is the axon action potential. (From J. M. R. Delgado, "Electrodes from Extracellular Recording and Stimulation," in *Physical Techniques in Biological Research,* edited by W. L. Nastuk, New York: Academic Press, 1964.)

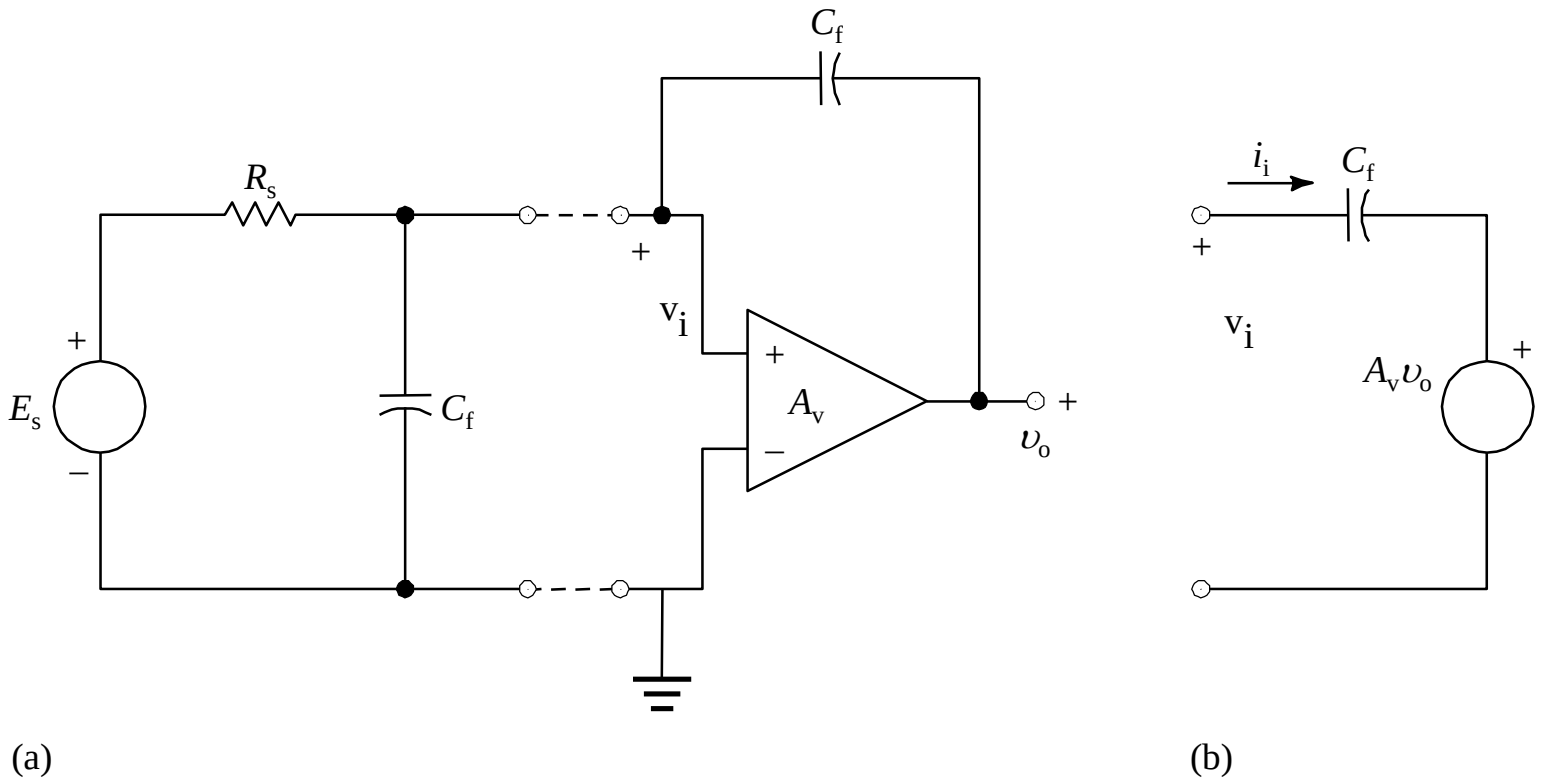

Figure 6.17 (a) Basic arrangement for negative-input capacitance amplifier. Basic amplifier is on the right-hand side; equivalent source with lumped series resistance R_s and shunt capacitance C_s is on the left. (b) Equivalent circuit of basic negative-input capacitance amplifier.

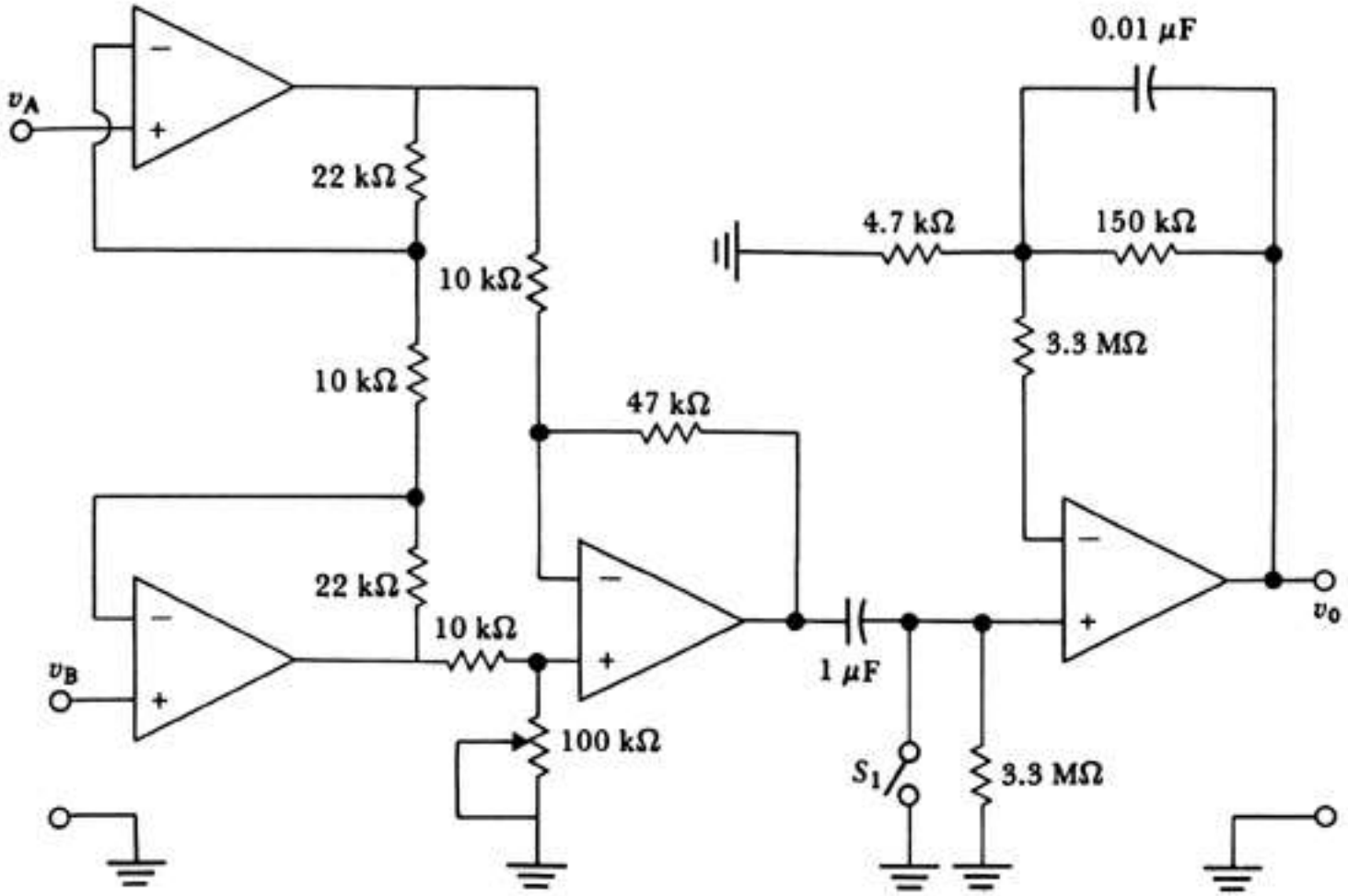

Figure 6.18 This ECG amplifier has a gain of 25 in the dc-coupled stages. The high-pass filter feeds a noninverting-amplifier stage that has a gain of 32. The total gain is 25 × 32 = 800. When μA 776 op amps were used, the circuit was found to have a CMRR of 86 dB at 100 Hz and a noise level of 40 mV peak to peak at the output. The frequency response was 0.04-150 Hz for ±3 dB and was flat over 4-40 Hz.

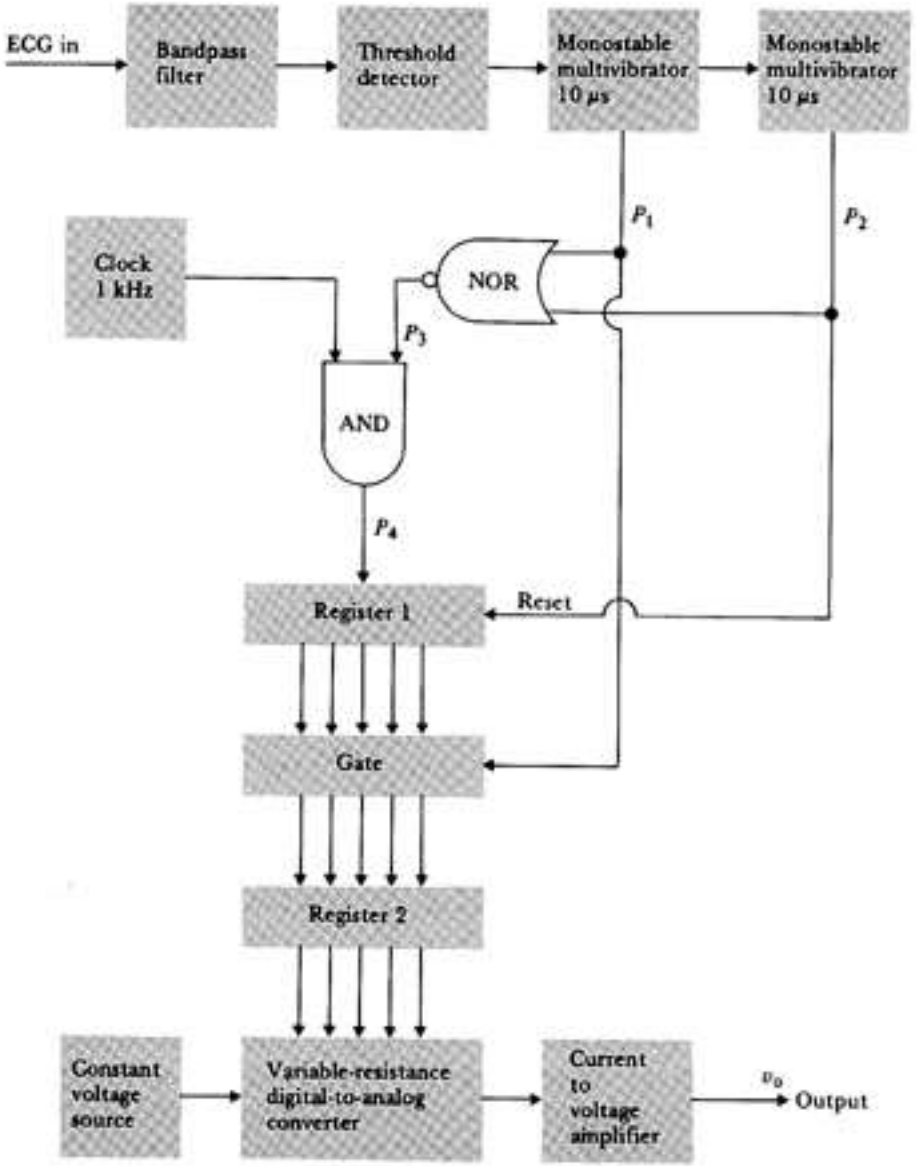

Figure 6.19 Block diagram of a beat-to-beat instantaneous cardiotachometer.

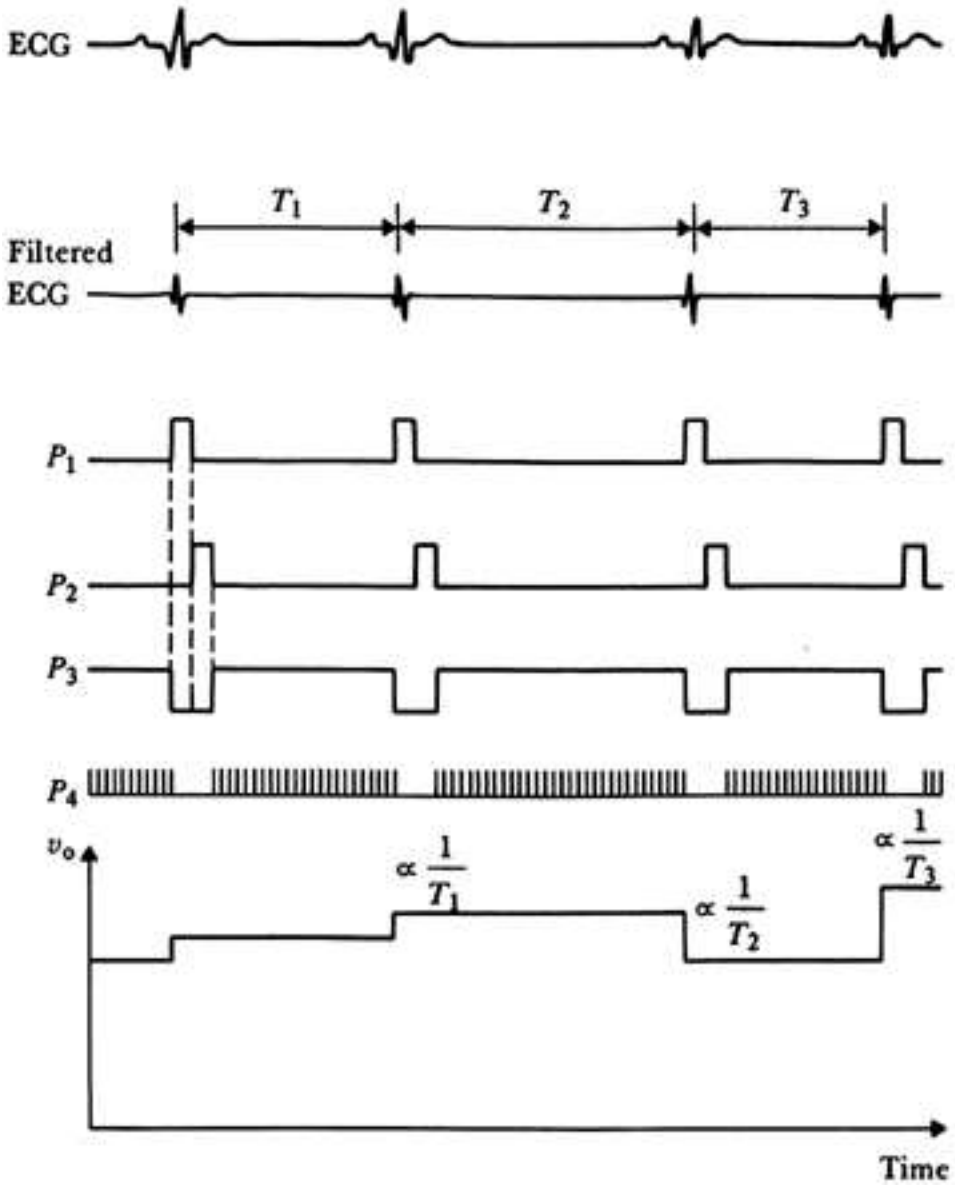

Figure 6.20 Timing diagram for beat-to-beat cardiotachometer in Figure 6.19.

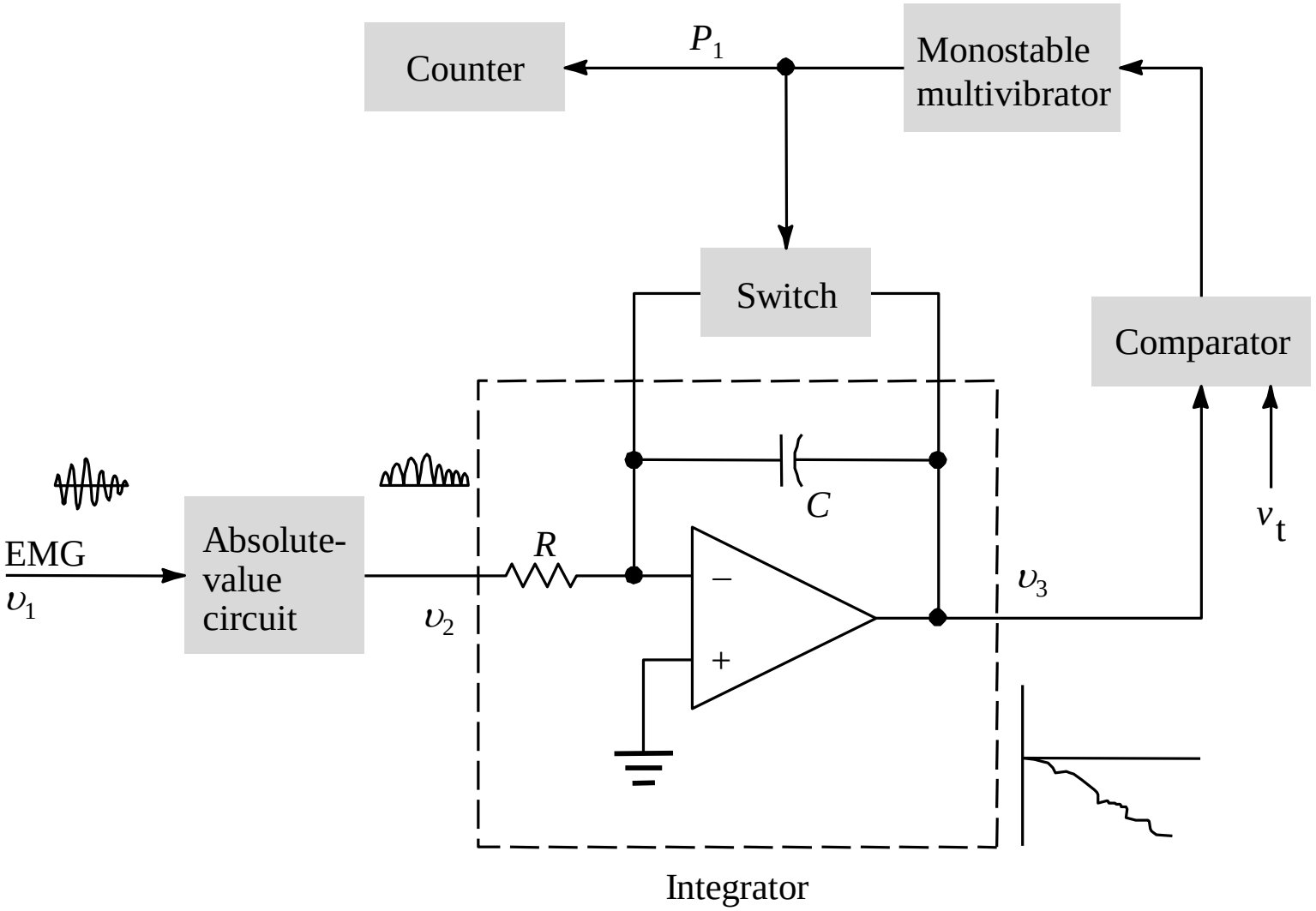

Figure 6.21 Block diagram of an integrator for EMG signals

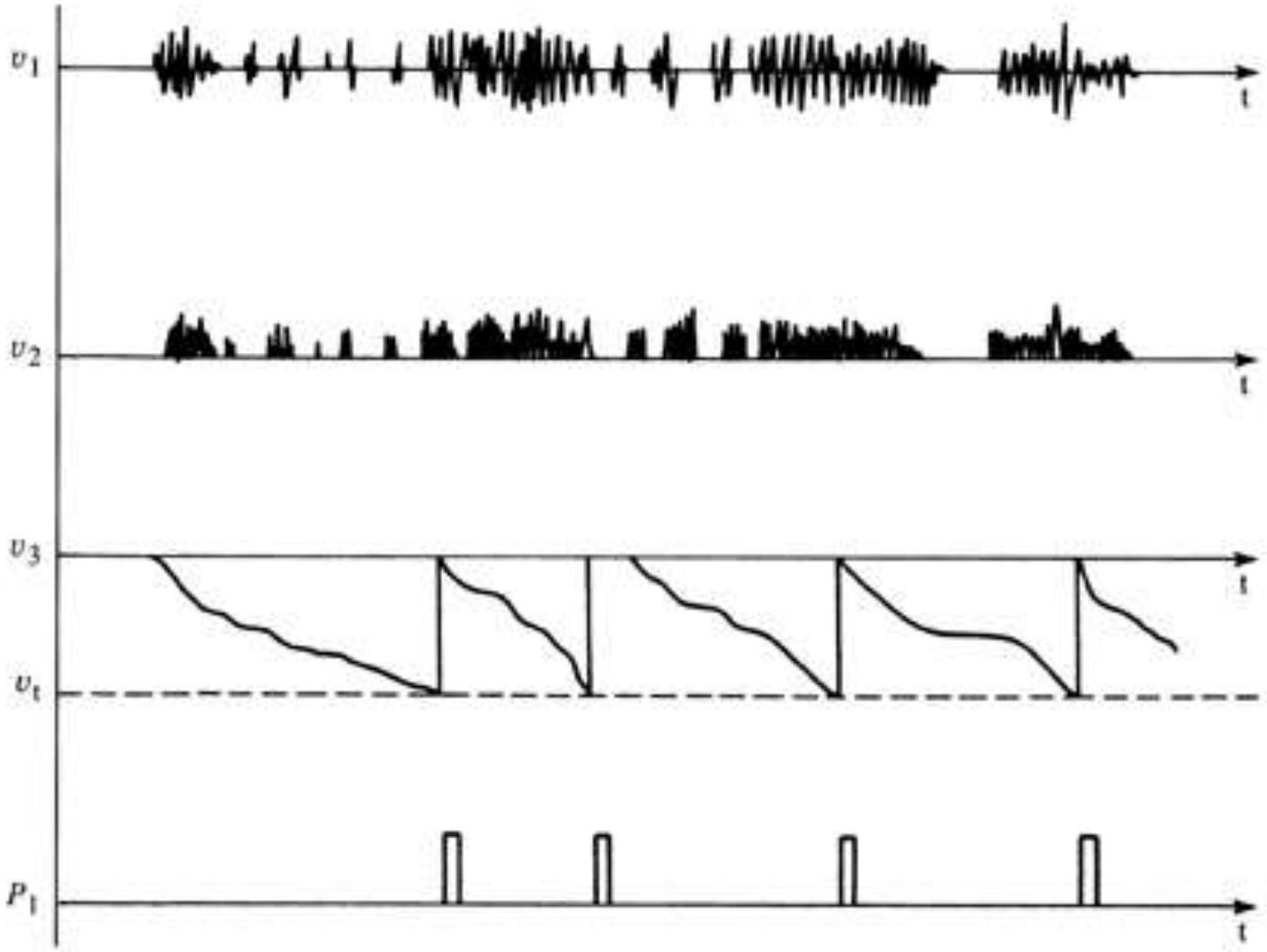

Figure 6.22 The various waveforms for the EMG integrator circuit shown in Figure 6.21

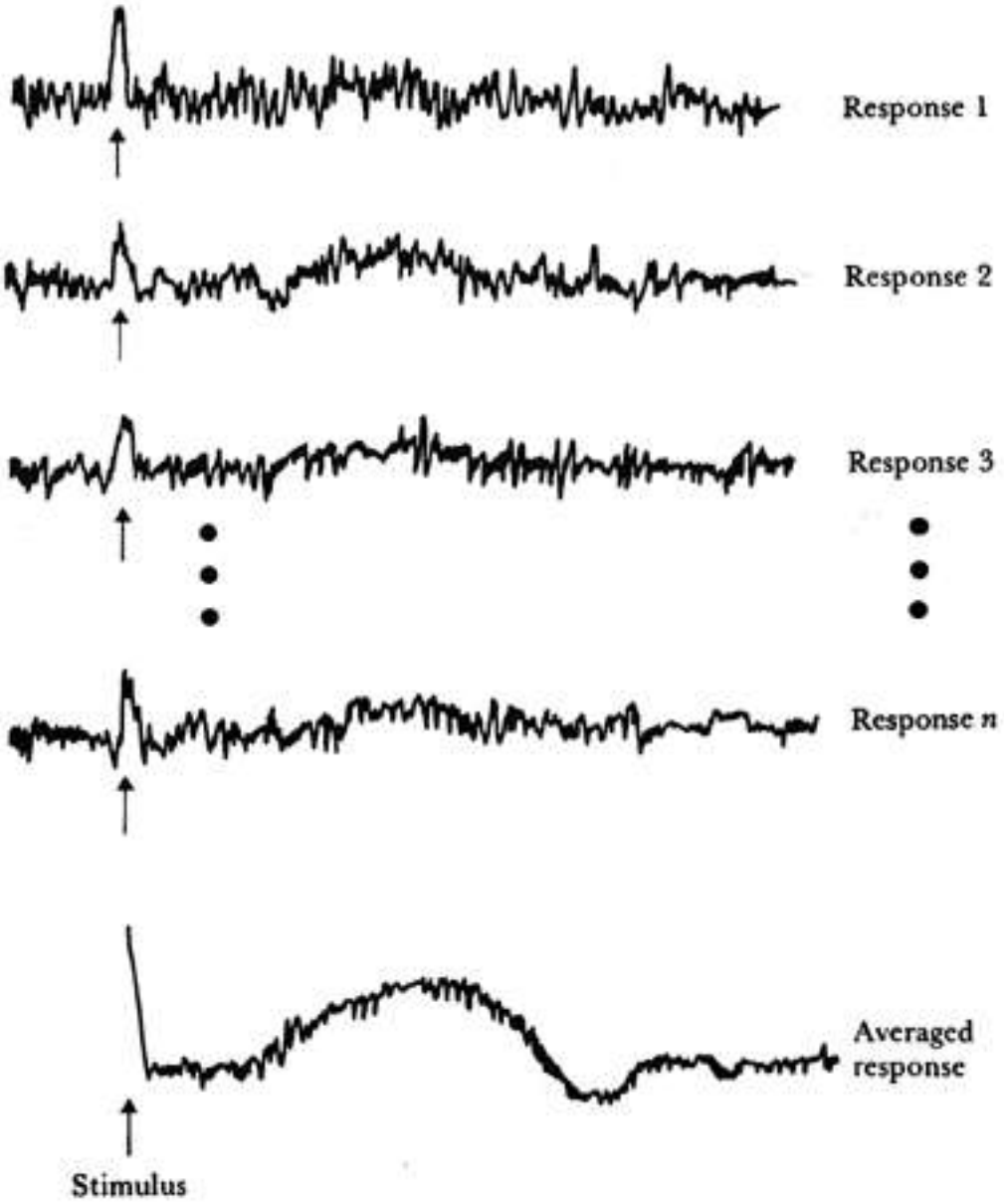

Figure 6.23 Signal-averaging technique for improving the SNR in signals that ware repetitive or respond to a known stimulus.

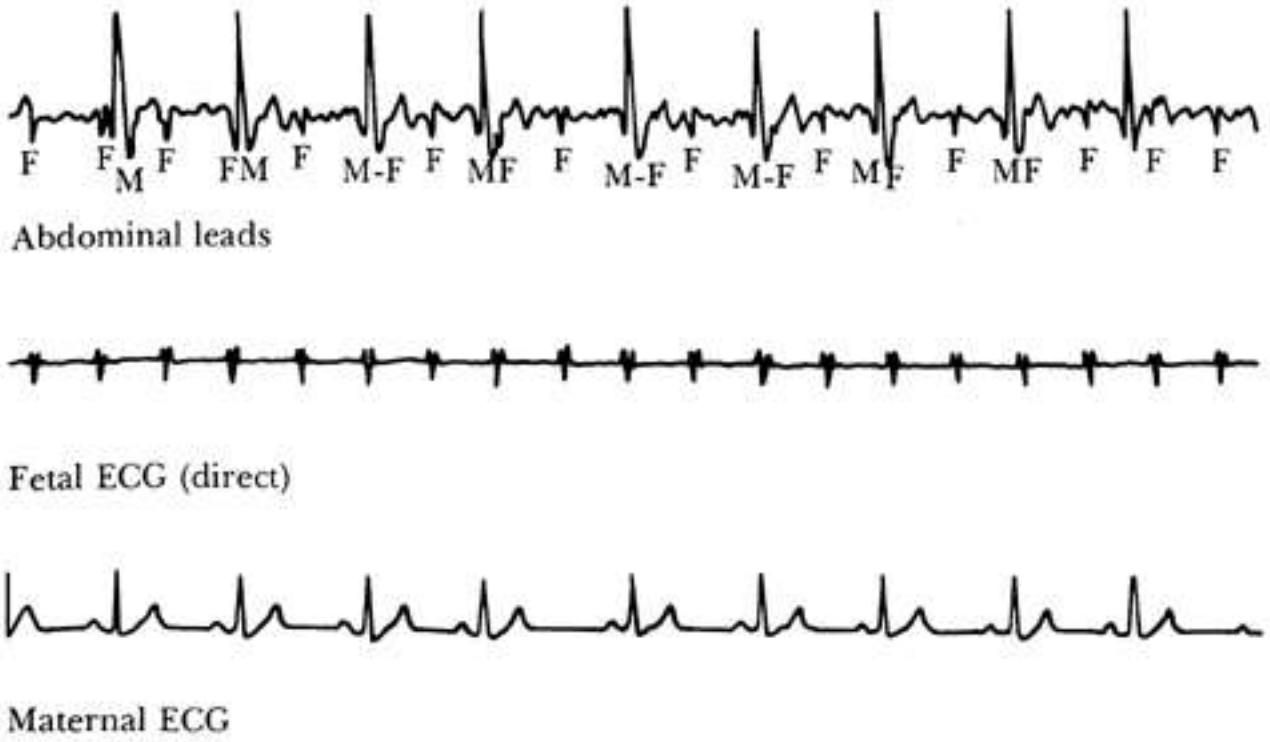

Figure 6.24 Typical fetal ECG obtained from maternal abdomen F represents fetal QRS complexes; M represents maternal QRS complexes. Maternal ECG and fetal ECG (recorded directly from the fetus) are included for comparison. (From "monitoring of Intrapartum Phenomena," by J. F. Roux, M. R. Neuman, and R. C. Goodlin, in CRC *Critical Reviews in Bioengineering,* **2,** pp. 119-158, January 197, © CRC Press. Used by permission of CRC Press, Inc.)

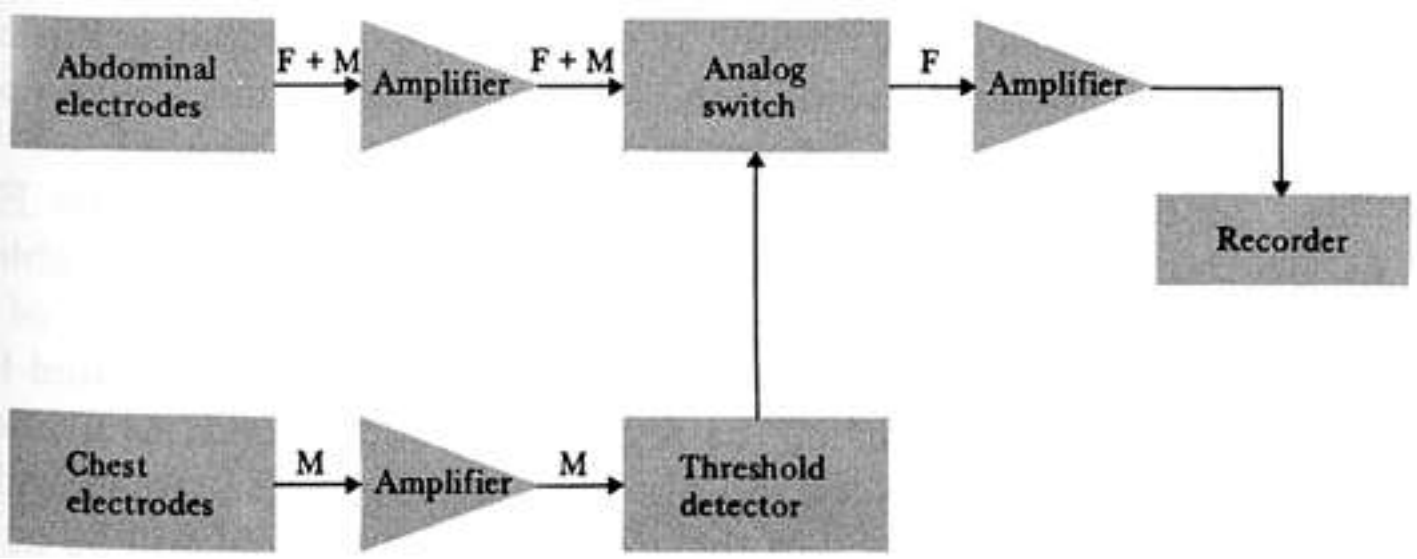

Figure 6.25 Block diagram of a scheme for isolating fetal ECG from an abdominal signal that contains both fetal and maternal ECGs. (From "monitoring of Intrapartum Phenomena," by J. F. Roux, M. R. Neuman, and R. C. Goodlin, in CRC *Critical Reviews in Bioengineering*, **2,** pp. 119-158, January 197, © CRC Press. Used by permission of CRC Press, Inc.)

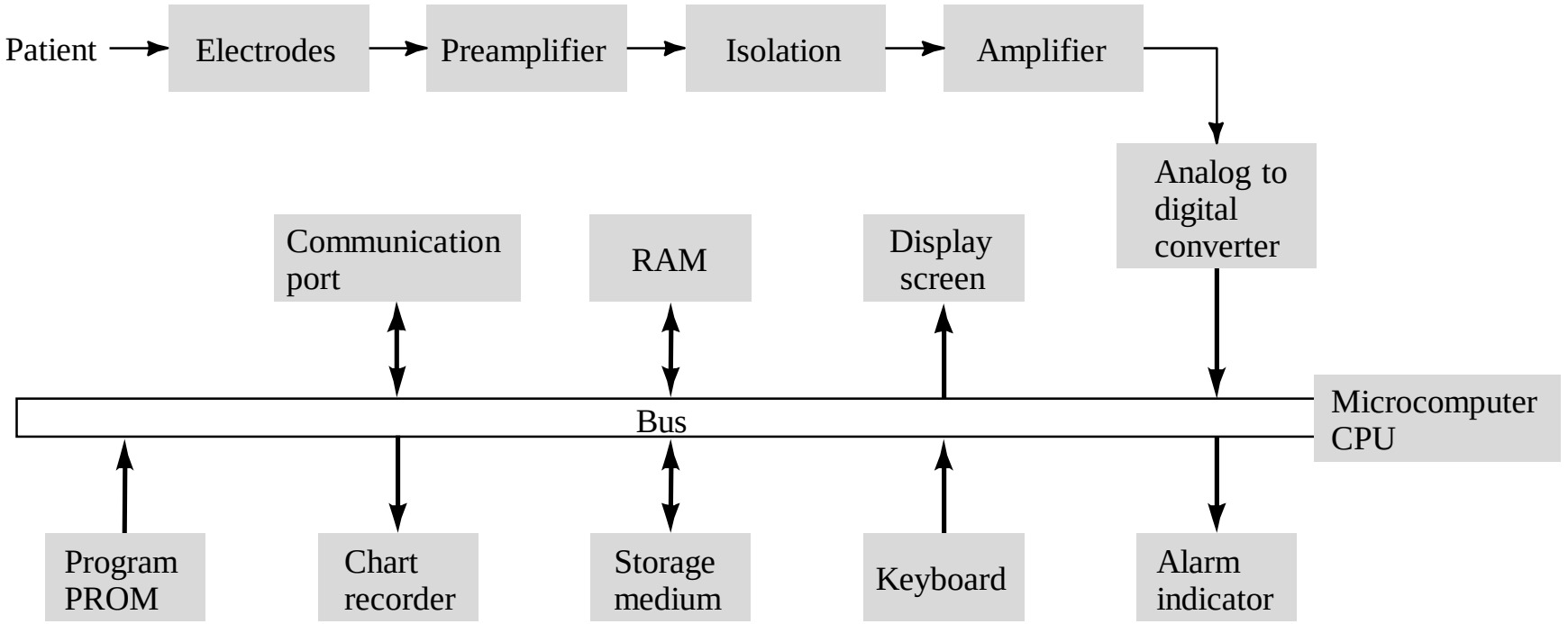

Figure 6.26 Block diagram of a cardiac monitor.

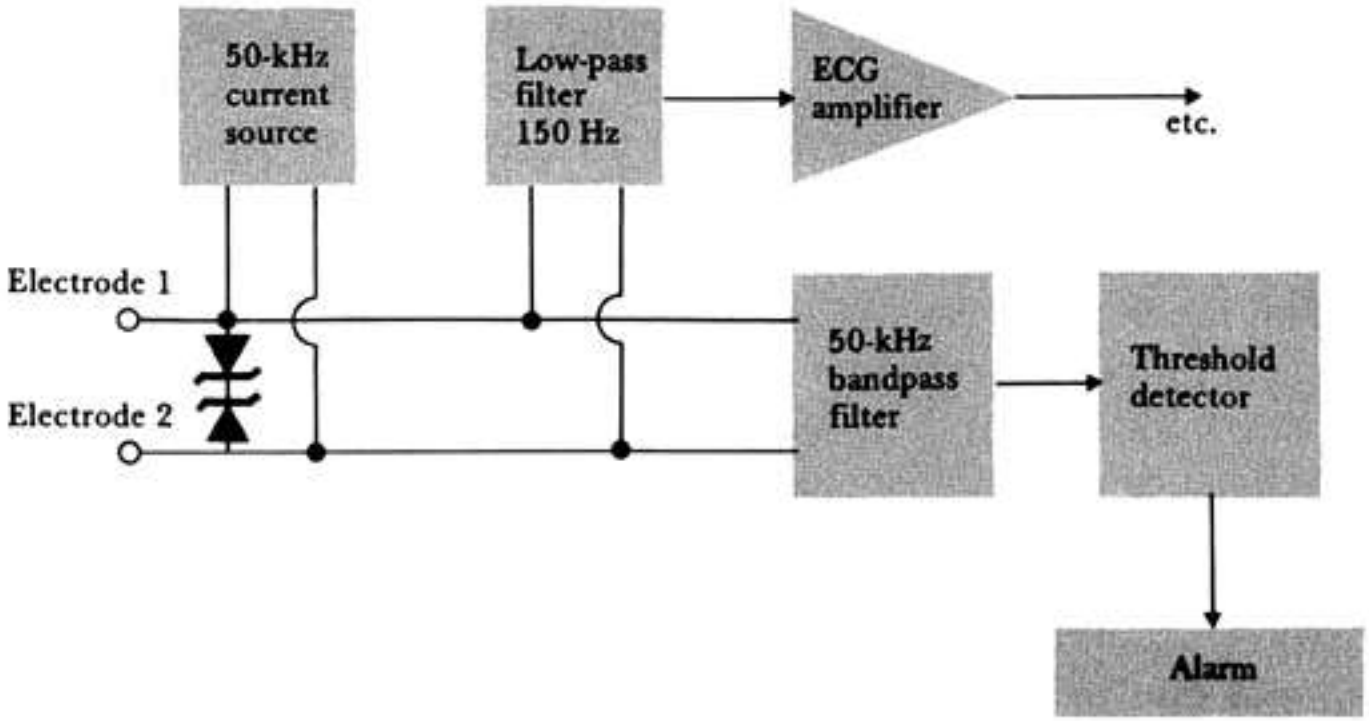

Figure 6.27 Block diagram of a system used with cardiac monitors to detect increased electrode impedance, lead wire failure, or electrode fall-off.

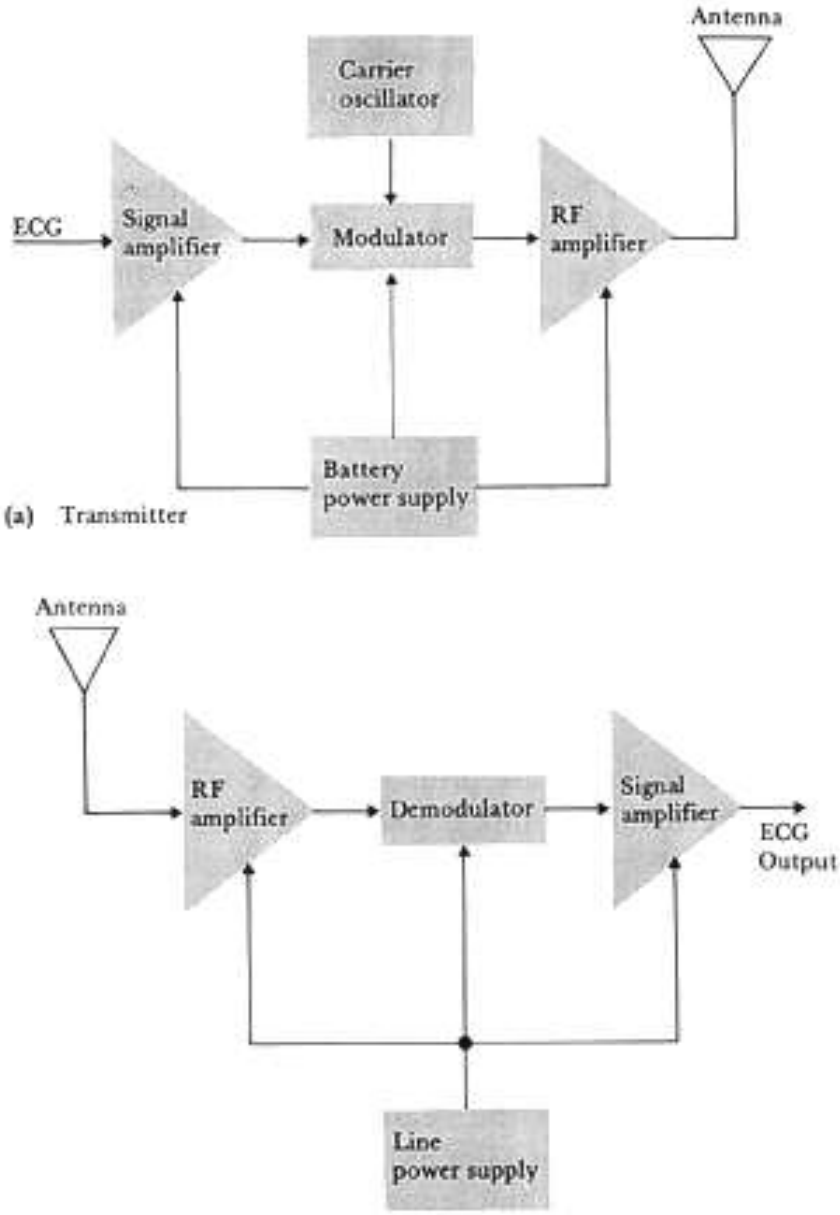

Figure 6.28 Block diagram of a single-channel radiotelemetry system

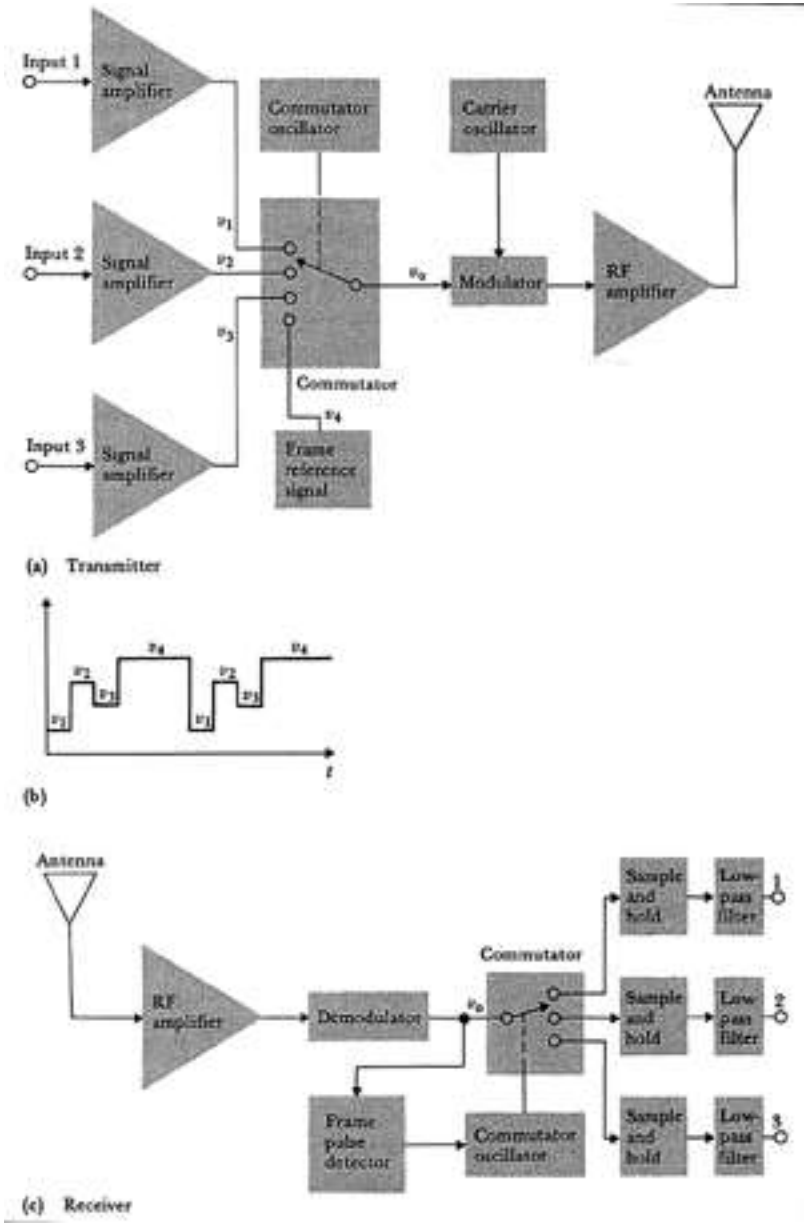

Figure 6.29 Block diagram of a three-channel time-division multiplexed radiotelemetry system (a) Transmitter. (b) Example of output waveform from commutator in transmitter. (c) Receiver.